Nanoscale

The uptake mechanism and biocompatibility of graphene quantum dots with human neural stem cells

Journal:	*Nanoscale*
Manuscript ID:	NR-ART-12-2013-006433.R1
Article Type:	Paper
Date Submitted by the Author:	18-Feb-2014

Complete List of Authors:	Shang, Weihu; Beijing Normal University, Department of Chemistry Zhang, Xiaoyan; Beijing Normal University, Key Laboratory of Cell Proliferation and Regulation Biology Zhang, Mo; Beijing Normal University, Department of Chemistry Fan, Zetan; Beijing Normal University, Department of Chemistry Sun, Ying; Beijing Normal University, Department of Chemistry Han, Mei; Beijing Normal University, Department of Chemistry Fan, Louzhen; Beijing Normal University, Department of Chemistry

Nanoscale

RSCPublishing

ARTICLE

The uptake mechanism and biocompatibility of graphene quantum dots with human neural stem cells

Cite this: DOI: 10.1039/xoxxoooooox

Weihu Shang, [a] Xiaoyan Zhang,[b] Mo Zhang, [a] Zetan Fan, [a] Ying Sun, [a] Mei Han* [a] and Louzhen Fan* [a]

Received ooth January 2013,
Accepted ooth January 2013

DOI: 10.1039/xoxxoooooox

www.rsc.org/

Cellular imaging after transplantation may provide important information to determine the efficacy of stem cell therapy. We have reported that graphene quantum dots (GQDs) are a type of robust biological labeling agent for stem cells that demonstrate little cytotoxicity. In this study, we examined the interactions of GQDs on human neural stem cells (hNSCs) with the aim to investigate the uptake and biocompatibility of GQDs. We examined the mechanism of GQDs uptake by hNSCs and investigated the effects of GQDs on the proliferation, metabolic activity, and differentiation potential of hNSCs. This information is critical to assess the suitability of GQDs for stem cell tracking. Our results indicated that GQDs were taken up into hNSCs in a concentration- and time-dependent manner *via* the endocytosis mechanism. Furthermore, no significant change was found in the viability, proliferation, metabolic activity, and differentiation potential of hNSCs after treatment with GQDs. Thus, these data open a promising avenue for labeling stem cells with GQDs and also offer a potential opportunity to develop GQDs for biomedical applications.

Introduction

Graphene, a two-dimensional honeycomb lattice of sp^2–carbon atoms,[1] has drawn intense attention for the plethora of applications in electronics, energy, materials, and biomedical areas, due to its unusual physicochemical properties.[2-5] Graphene quantum dots (GQDs) are one of the most important graphene derivatives and have ignited tremendous research interest in recent years.[6-16] With its superiority in terms of chemical inertness, stable photoluminescence, high water solubility, better surface grafting, and low cytotoxicity, GQDs are excellent candidates for use in bioimaging and biosensing applications. [10,17-23]

Stem cells are a population of immature tissue precursor cells that can self-renew to produce more stem cells and can differentiate into diverse specialized cell types. Advances in stem cell research have provided an important understanding of the stem cell biology and have offered significant potential for the development of new strategies for the treatment of intractable conditions, such as neurological diseases, cancer, spinal cord injury, cardiac disease, type I and II diabetes, liver disease, and bone disease.[24-32] Human neural stem cells (hNSCs) are self-renewing, multipotent cells that generate the main phenotypes of the nervous system.[33] Furthermore, hNSCs regeneration of damaged brain tissue represents a promising strategy for the treatment of neurological disorders,[24,34,35] including Parkinson's disease, Alzheimer's disease, stroke, and spinal cord lesions, among other diseases. However, to monitor the survival, migration, differentiation, and regenerative effect of stem cells after transplantation, it has become desirable to label these cells to understand how they behave and to understand their biological functions in the body.[36,37]

Until recently, several nanoparticles have been used to label stem cells,[38-45] which mainly include magnetic nanoparticles (MNPs) and quantum dots (QDs).[34,46] However, due to stem cell division or the transfer of MNPs to other cells, the detected signal of MRI decreases by the dilution of MNPs. Thus, it has become difficult to correlate the signal with the injected cell number. Most traditional QDs contain heavy metal elements (such as Cd^{2+}, Pb^{2+}, etc.), which are released from QDs, and can induce potential cytotoxicity in biological systems.[38] On the basis of the latest non-human primate study, most of the intravenous injection doses of cadmium have remained in the liver, spleen, and kidneys after 90 days.[47] In addition, in most cases, efficient internalization of such nanoparticles requires the use of excipient or specific peptides.[38,48] Problems with detections and toxicities have emphasized the need for new sources of stem cell imaging.

In our previous study, we successfully prepared fluorescent GQDs, in the absence of any coating or conjugation with macromolecules and have directly and efficiently used as bioimaging probes for the labeling of stem cells.[17] In addition, GQDs also exhibit little cytotoxicity, where 100 μg/ml GQDs did not significantly weaken cell activity as detected using the MTT assay.[17]

However, given the promise of hNSCs in regenerative medicine and the GQDs perspective, the interactions between them are still largely unknown. Herein, the present study was designed to investigate the cellular response of GQDs to hNSCs. The cellular uptake mechanisms, internalization, and retention of GQDs were analyzed using confocal microscopy and transmission electron microscopy (TEM) observation. The cellular responses of GQDs on the ability of hNSCs to self-renew and differentiate were estimated using immunocytochemistry. The findings presented in this study provide information on the quantification and mechanism of GQDs in cellular uptake and show that the GQDs demonstrate good biocompatibility under a common dose and exhibit great potential applications in biolabeling, particularly in the bioimaging of stem cells.

Results and discussion

Quantification of GQDs uptake

GQDs have been previously demonstrated to directly and easily penetrate into hNSCs using confocal microscopy.[17] To confirm this microscopic observation and to determine the efficiency of GQDs uptake, we first used a microplate reader to detect the fluorescence intensity of GQDs dissolved in PBS. The GQDs were strongly emissive with an excitation wavelength at 360 nm and emission wavelength at 535 nm. As shown in Fig. 1A, the photoluminescence (PL) intensity produced by the GQDs correlated highly with the GQDs concentrations (1-100 μg/ml) (R^2=0.9948), which indicated that it was a precise and reliable method to quantify the GQDs.

After the hNSCs were incubated with varying concentrations of GQDs (20-500 μg/ml) for 24 h, the resulting fluorescence was measured using the microplate reader. As shown in Fig. 1B, there was a dose dependent increase of fluorescence intensity at 20-200 μg/ml, although the fluorescence intensity at 100 μg/ml was slightly higher than 50 μg/ml, suggesting that the GQDs were taken up by hNSCs in a dose-dependent manner. On the other hand, at the highest concentration tested (500 μg/ml), there was no significant difference compared with 200 μg/ml, indicating that possible saturation of the uptake was achieved at 200 μg/ml. To determine the uptake kinetics, hNSCs were incubated with 50 μg/ml GQDs for different time periods and then collected, washed, lysed, and measured using the microplate reader. These data, which are presented in Fig. 1C, demonstrated that the GQDs uptake occurred in a time-dependent manner. As the incubation time increased, more GQDs were detected. Within 3 h, we were able to detect significant uptake, and the GQDs uptake was relatively rapid.

Mechanism of GQDs uptake by hNSCs

Next, we performed a primary investigation of the cellular uptake mechanism and pathway for GQDs. Endocytosis is known as a general entry mechanism for various extracellular materials and is an energy-dependent uptake mechanism that is

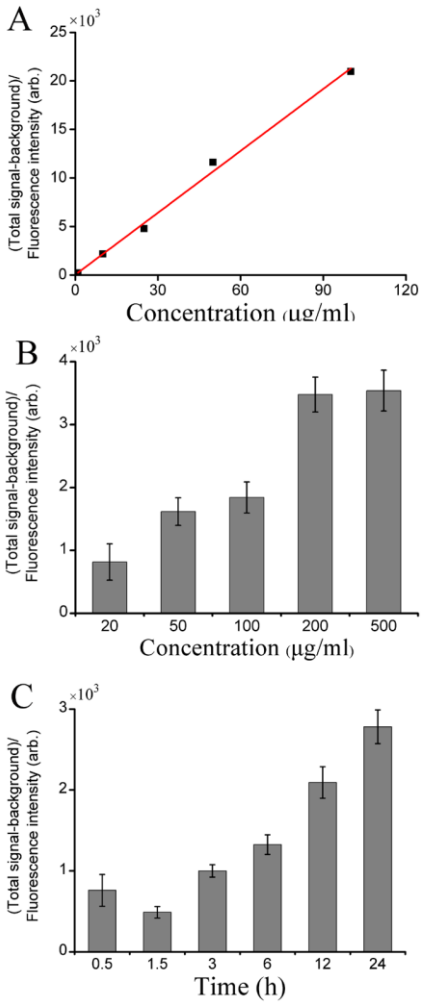

Fig. 1 Quantification and kinetics of GQDs uptake. (A) The PL intensity produced by GQDs was observed to be linearly dependent on the concentration (R^2=0.9948), with an excitation wavelength at 360 nm and emission wavelength at 535 nm. (B) The fluorescence intensity for all GQDs concentrations tested on hNSCs. (C) The fluorescence intensity for 50 μg/ml GQDs incubated in hNSCs for different time periods. The values are expressed as the mean ± SD (n = 3).

hindered when incubations are carried out at low temperatures (4°C instead of 37°C) or in ATP (adenosine triphosphate)-depleted environments.[49] Cellular incubations with GQDs were performed at 4 °C or pretreated with 50 mM 2-deoxy-D-glucose and 25 mM NaN_3 for 45 min. Treatment with NaN_3 is known to disturb the production of ATP in cells, thus blocking the endocytic pathway.[50]

Indeed, compared with the 37°C condition (Fig. 2A), the fluorescence levels observed using confocal microscopy of cells after GQDs incubation at 4°C (Fig. 2B) or ATP depletion by 2-deoxy-D-glucose and NaN_3 (Fig. 2C) were low. This was verified by fluorescence measurements, which indicated a significant reduction in fluorescence intensity at 4 °C or under the ATP depletion conditions (Fig. 3). The results showed that GQDs entry into hNSCs was ATP- and temperature-dependent. Moreover, cell uptake of GQDs by hNSCs was further confirmed using TEM. As shown in Fig. 4, the GQDs were

indeed internalized by hNSCs and were located in the cytoplasm. This result is consistent with the results obtained by Markovic's group, in which they found that internalization of GQDs in U251 cells occurred *via* an endocytosis mechanism after the cells were incubated with photoexcited GQDs for 12 h using TEM assay.[51]

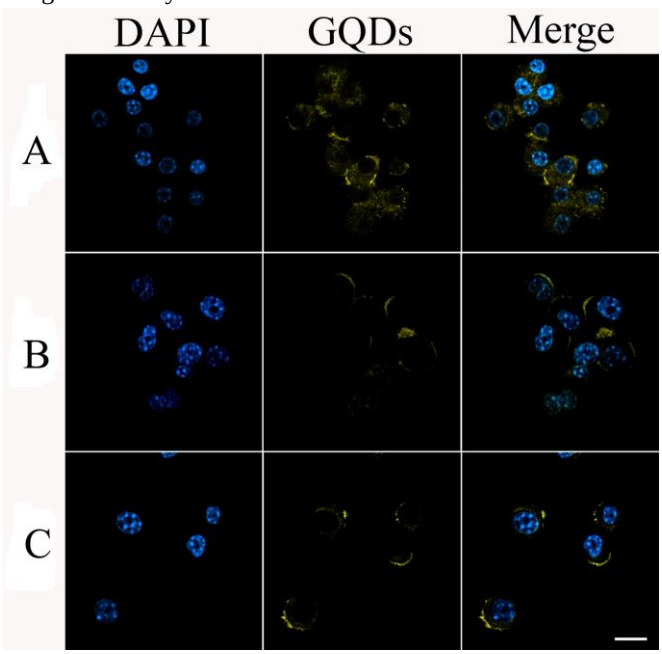

Fig. 2 Confocal microscopy images of hNSCs after incubation with GQDs at (A) 37°C, (B) 4°C, and (C) after pretreatment with 2-deoxy-D-glucose and NaN_3 (The scale bar = 20 μm).

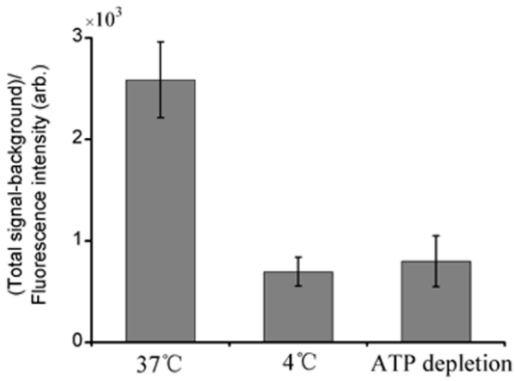

Fig. 3 The fluorescence intensity for 25 μg/ml GQDs incubated in hNSCs for 24 h in different conditions, including 37°C, 4°C and ATP depletion pretreated with 2-deoxy-D-glucose and NaN_3. The values are expressed as the mean ± SD (n = 3).

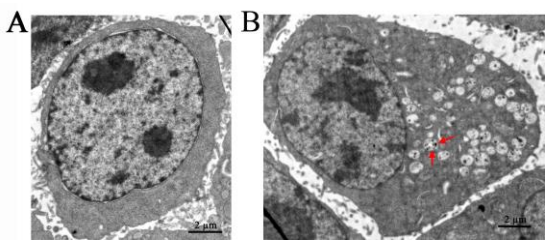

Fig. 4 TEM images of hNSCs after 24 h incubation with 25 μg/mL of GQDs. (A) Control, (B) GQDs. Red arrows in (B) indicate intracellular vesicles engulfing GQDs.

Referring to the work conducted by Markovic *et al.* and combined with our results, we suggested that the potential mechanism for GQDs entry into stem cells was the endocytosis, which internalized cargo in transport vesicles. The endocytosis of nanoparticles by cells may occur *via* two major mechanisms, including phagocytosis and pinocytosis.[52] Phagocytosis is a type of macroscale endocytosis that is the uptake of large particles by only some specialized mammalian cells such as macrophages, monocytes, and neutrophils. Pinocytosis is the uptake of small particles. Furthermore, receptor-mediated endocytosis is a process by which cells internalize molecules (endocytosis) by the inward budding of plasma membrane vesicles containing proteins with receptor sites specific to the molecules being internalized. The insulin-conjugated GQDs were reported to internalize in 3T3-L1 adipocytes through receptor-mediated endocytosis containing insulin receptors.[20] Besides, Wang *et al.* reported that titanium dioxide nanoparticles also entered into neural stem cells *via* a receptor-mediated endocytosis pathway.[53]

Zhang *et al.* first confirmed that carbon nanomaterials (including carbon nanotubes, nanodiamond, and graphene) could be taken up by HeLa cells using TEM and that they were located in the cytoplasm, such as in lysosomes, mitochondria, and endoplasm.[54] In addition, Wang and colleagues reported the effects of graphene oxides (GOs) on human fibroblast cells. They found that GOs entered into the cytoplasm *via* the endocytosis pathway and were mainly located in lysosomes, mitochondria, endoplasm, and the cell nucleus. However, after entering into the cytoplasm, GOs might disturb the course of cell energy metabolism and gene transcription and translation and subsequently result in cell apoptosis or death.[55] These results clearly showed that GQDs could readily gain access to hNSCs, and then entered presumably into hNSCs in an energy-dependent manner *via* receptor-mediated endocytosis pathway.

Cellular retention

As a type of useful cell tracking agent, it is important that a proportion of the cells within the population retain their label throughout the time course of the experiment. To investigate the cellular retention of GQDs, hNSCs were incubated with 25 μg/ml GQDs for 48 h, and the culture medium was changed to normal culture medium in the absence of GQDs and cultured for 1, 3, 5, 7, and 9 days. As shown in Fig. 5, there was a robust loading of the hNSCs 48 h after incubation of cells with GQDs (Fig. 5a). By day 1 (Fig. 5b), the proportion of labeled cells was similar to control-day 0 (Fig. 5a); but by day 3 (Fig. 5c), the percentage of labeled hNSCs was noticeably reduced. With increasing incubation days, the fluorescence signals in the cells were slightly decreased (Fig. 5d-f). On one hand, the gradual decrease could be due to the rapid division of hNSCs, the doubling time was approximately 33 h. Kim *et al.* reported that NPs internalized by cells were split between daughter cells during the parent cell division.[56] On the other hand, this gradual decrease might be due to GQDs excreted from cells, causing a dilution of the GQDs signal.[57] To further characterize the exocytosis of GQDs, we quantified the fluorescence intensity

over time by the microplate reader (Fig. 6). The results showed that the percentage of labeled hNSCs had decreased to approximately 93%, 56%, 36%, 27%, and 15% by day 1, 3, 5, 7, and 9, respectively. To the best of our knowledge, many nanoparticle vectors for stem cell labeling or tracking have a significant limitation, specifically poor retention. Aleksandra and colleagues reported that approximately 85% of both mouse embryonic stem cells and kidney stem cells were labeled by QDs at day 0, but by day 3, the percentage of labeled stem cells had decreased to 10% and 40%, respectively.[46] In addition, Wu *et al.* reported that by day 4, the percentage of positive cells had decreased to ~4%, and by day 7, the percentage of positive cells was only ~0.7% using FACS analysis.[41] Taken together, our GQDs were only suitable for relatively short-term tracking, which motivates the development of newer nanoparticle vectors for long-term tracking.

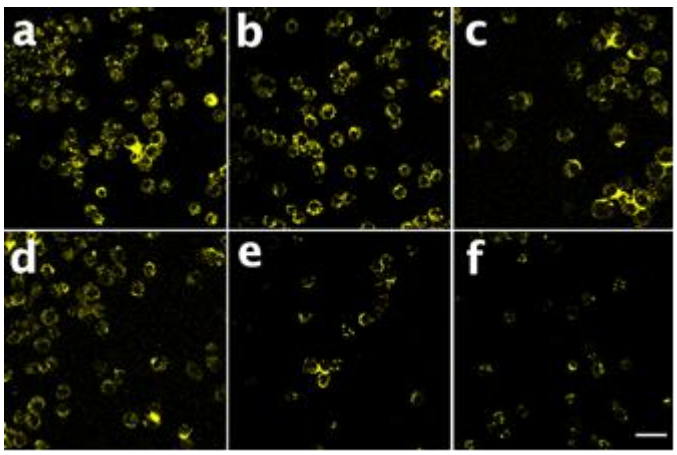

Fig. 5 Retention of fluorescent signals of GQDs in hNSCs. Cells were incubated with GQDs for 48 h at 25 μg/ml (a), and the media were replaced with culture medium without GQDs and cultured for 1 day (b), 3 days (c), 5 days (d), 7 days (e), and 9 days (f). Scale bar, 20 μm.

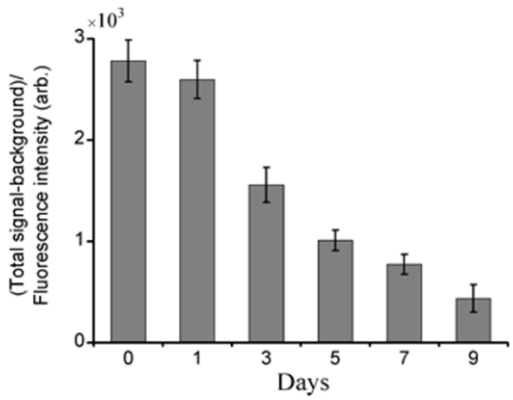

Fig. 6 The fluorescence intensity of GQDs in hNSCs. Cells were incubated with 25 μg/ml of GQDs for 48 h, and the media were replaced with culture medium without GQDs and cultured for 0, 1, 3, 5, 7, and 9 days. The values are expressed as the mean ± SD (n = 3).

Effect of GQDs on hNSCs proliferation and cell viability

To develop applications of GQDs in stem cells, it was necessary to investigate the biocompatibility of GQDs in stem cells. To investigate if GQDs had any effect on population growth, the number of hNSCs was quantified over a 3-day period. GQDs labeling had no effect on the population growth when compared to unlabeled controls (Fig. 7A). Furthermore, to examine the effect of GQDs on the proliferation of hNSCs, we used the CellTiter-Glo™ assay, which is an adenosine triphosphate (ATP)-based cell proliferation assay that provides an accurate count of the number of cells.[58] After treatment for 24, 48 and 72 h, no significant decrease in the cell viability was observed in hNSCs as compared to controls, suggesting that a 72-hour exposure to 200 μg/ml GQDs had no significant effect on cell viability of hNSCs (Fig. 7B).

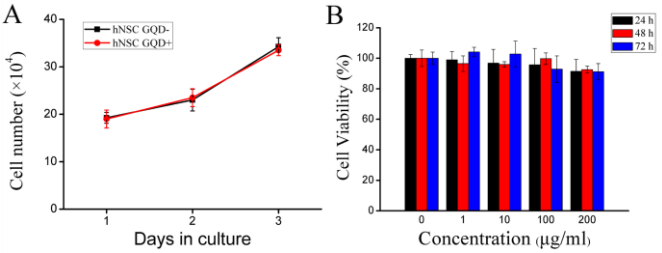

Fig. 7 Population growth and cell viability following GQDs labeling. (A) Population growth curves for unlabeled control hNSC (hNSC GQDs-) and GQD-labelled hNSC (hNSC GQDs+). (B) The cell viability measured using the ATP assay for different GQDs concentrations and at different culture times; n = 3 for each experiment.

Effect of GQDs on hNSCs self-renewal capacity

To further investigate whether GQDs affected the self-renewal ability of hNSCs, cells were incubated with 25 μg/ml GQDs for 48 h, and then the GQDs-labeled hNSCs were collected and dissociated into single cells. Next, one cell was cultured per well *in vitro*. Finally, the initial cells formed large neurospheres, and the cells expressing the cell type-specific marker for hNSCs, nestin, were identified (Fig. 8). We found that GQDs did not affect the self-renewal capacity of hNSCs.

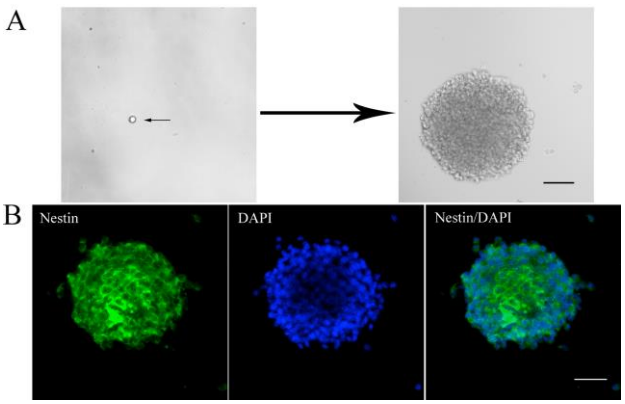

Fig. 8 GQDs do not affect the self-renewal ability and expression of the cell type-specific marker in hNSCs. (A) GQDs-labeled hNSCs were dissociated into single cells, as showed with the black arrow and the single cell formed large neurospheres after 12 days in normal culture medium. (B) Immunofluorescent staining for nestin protein in the neurospheres showed nestin-positive cells (green). Nuclei are stained with DAPI (blue). Scale bar, 50 μm.

Effect of GQDs on hNSCs metabolic activity

Having demonstrated that GQDs had no detectable effect on hNSCs proliferation and the capacity of self-renewal, we next examined GQDs effects on metabolic activity. An AlamarBlue™ assay was employed to measure the metabolic activity of the cells according to a previously reported method.[59] As shown in Fig. 9, the cell metabolic rate appears to be nearly the same when exposed to the tested concentrations (0-250 μg/ml). There was no significant difference compared with control, which predicated that that GQDs had no profound effects on hNSCs metabolic activity *in vitro*.

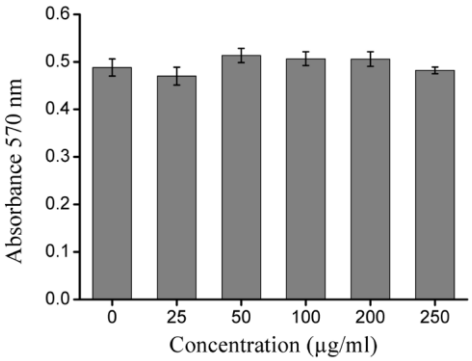

Fig. 9 Cell metabolic activity in the presence of GQDs at various concentrations ranging from 0 μg/ml to 250 μg/ml. The error bars represent the standard deviation of the mean (n = 3). There was no statistically significant difference compared with control.

GQDs do not affect the differentiation potential of hNSCs

Finally, we sought to determine whether GQDs disrupted the differentiation potential of hNSCs. The differentiation of hNSCs was initiated by exchanging the culture media with media containing 10% FBS, in the absence of the growth factors bFGF and EGF. During the differentiation process, hNSCs differentiated into neurons and glia, which supported the activity of neurons (Fig. 10).[60] After 14 days of differentiation, we could not detect any difference in the hNSCs growth between the control group and the 25 μg/mL GQDs treatment group (Fig. 10A and B). Cells from both groups showed elongated cell shapes with neurite outgrowths, resulting in the formation of an interconnected neuronal network.[60,61] In addition, glial fibrillary acidic protein (GFAP) and neuron-specific class III beta-tubulin (tubulin βIII) were examined using immunocytochemistry. As shown in Fig. 10, hNSCs could spontaneously differentiate into neurons and glial cells (Fig. 10C-F). For quantitative analysis, tubulin βIII- and GFAP-positive cells were quantified in a visual field (approximately 0.3 mm^2, over 200 cells per area) at 200×. The results are expressed as a percentage of the total cells as indicated by DAPI staining. There were no significant differences for the percentages of neurons or glial cells to the total cells between the two groups (Fig. 10G and H). Thus, the results indicated that GQDs treatment did not affect the percentages of either neurons or glial cells.

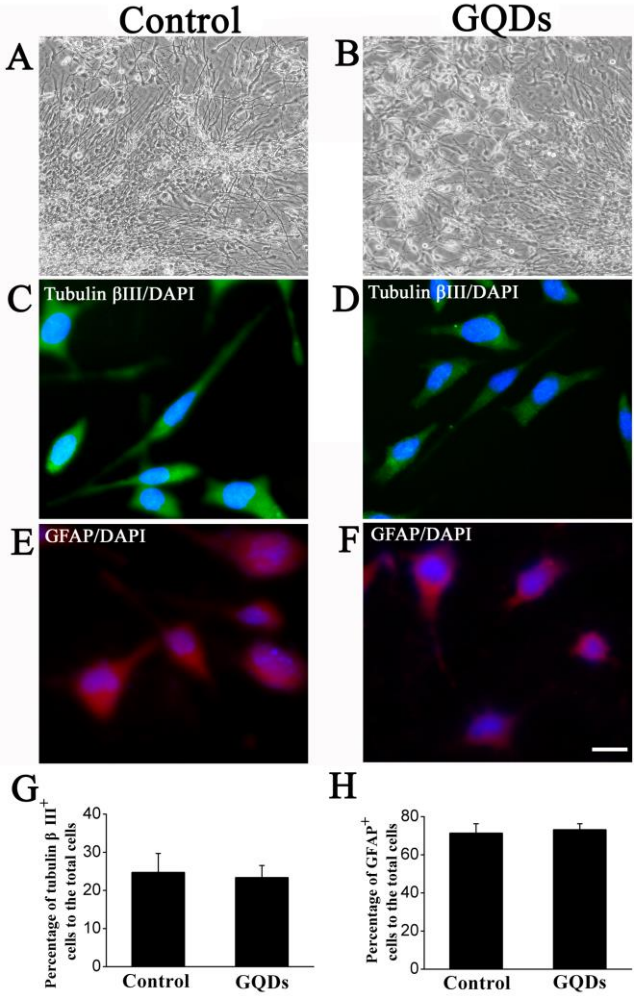

Fig. 10 GQDs do not affect the differentiation potential of hNSCs. Bright-field images of the hNSCs differentiated for 14 days (A: control; B: 25 μg/mL GQDs). Representative microphotographs demonstrated tubulin $βIII^+$ (green, C, D) and $GFAP^+$ (red, E, F) cells. The nuclei were counterstained with DAPI (blue). Scale bar, 20 μm. Panels (G) and (H) show the percentages of tubulin βIII- and GFAP-positive cells relative to the total DAPI-positive cells. The error bars represent the standard deviation of the mean (n = 3). There was no statistically significant difference compared with the control.

Experimental section

Quantification of GQDs

GQDs were prepared from high purity graphite rods according to a facile electrochemical method as previously reported.[17] To measure the fluorescence intensity of GQDs, we prepared a series of standard solutions of GQDs (1, 5, 10, 20, 25, 50, and 100 μg/ml). The fluorescence intensity of GQDs was measured using a Victor^3 V 1420 Multilabel reader (PerkinElmer, USA) and calculated to plot a calibration curve of fluorescence intensity vs the concentration of GQDs. The excitation wavelength was 360 nm, and the emission wavelength was 535 nm.

Cell culture

The hNSCs were maintained in DMEM/F12 medium supplemented with 20 ng/ml bFGF, 20 ng/ml EGF, 2% B27, 100 IU/ml penicillin, and 100 IU/ml streptomycin in a 5% CO_2 humidified atmosphere at 37°C as previously described. The medium was refreshed every 2 or 3 days. The cells were passaged by gently triturating the resulting neurospheres into a quasi-single cell suspension once per week. All hNSCs experiments were performed between passages 6 and 10. Neural differentiation could be initiated by adding 10% FBS and removing growth factors (bFGF and EGF) from the culture media. The cells were allowed to differentiate for 7 to 14 days.

Intracellular uptake

The cells were seeded onto 384-well plates at 2×10^4 cells/ml overnight. Different concentrations of GQDs (20, 50, 100, 200, and 500 μg/ml) were added, and the plates were incubated at 37°C for 24 h. After incubation, the supernatant was removed and the cells were washed with 0.1 M PBS solution three times to remove residual GQDs and wash off GQDs attached to surface of hNSCs. Subsequently, lysis buffer (0.1% NH_4Cl and 10% dodecyl phenyl sodium sulfonate solution) was added to each well, and the plates were incubated overnight at 37°C. The fluorescence intensity of GQDs was detected using a microplate reader.

Confocal imaging

To observe the cellular retention of GQDs, confocal laser scanning microscopy (CLSM) was used. Cells were incubated with 25 μg/ml GQDs on a cover glass incubated with PLA on culture plates. The cells were fixed with 4% paraformaldehyde and observed using a confocal laser-scanning microscope (FV300/IX70, Olympus America Inc.).

Transmission electron microscopy observation

To analyse the course of endocytosis and intracellular localization, hNSCs were treated with 25 μg/mL GQDs and cultured in a humidified 5% CO_2 balanced air incubator at 37°C for 24 h. The cells were fixed with 2.5% glutaraldehyde solution and embedded with epoxy resin, resulting in an ultrathin cell specimen that was observed using TEM.

Cell viability assay

The cell viability was determined using the CellTiter-Glo™ Luminescent cell viability reagent (Promega, Madison, WI) on 384-well plates according to the manufacturer's instructions. Briefly, neurospheres were dissociated to single cells and seeded onto 384-well plates at 2×10^4 cells/ml overnight. Different concentrations of GQDs (1-200 μg/ml) were added, and the plates were incubated at 37°C for 24, 48 and 72 h. The detection protocol included the addition of 10 μl of working solution of the ATP kit to each well. The luminescence of each well was measured using a Victor^3 V Multilabel reader (PerkinElmer, USA).

AlaramBlue™ assay

An AlamarBlue™ assay was employed to measure the metabolic activity of the cells as previously described.[59] Briefly, 3000 hNSCs/cm^2 were seeded per well of a 96-well plate for 24 h and then exposed to 0, 25, 50, 100, 200, and 250 μg/ml GQDs for an additional 24 h. The medium was changed every 48 h. After 6 days, the cells are washed twice with PBS, and dye was added to the cells, resulting in a color change of the solution from blue to pink. The absorbance was measured using a microplate reader.

Immunocytochemistry

An immunocytochemistry assay was performed according to the manufacturer's protocol. After differentiation, hNSCs were fixed for 15 min in 4% paraformaldehyde, permeabilized with 0.1% Triton X-100 in PBS solution for 30 min, and then blocked with PBS containing 0.1% Triton X-100 and 1% BSA at room temperature for 1 h. The cells were incubated overnight at 4°C in the following primary antibodies: anti-tubulin βIII (similar to TUJ1) (1:200; clone TU-20, Millipore, CA, USA) and anti-GFAP (1:1000; Millipore, CA, USA). The cells were then washed with PBS three times and incubated with either goat anti-mouse FITC (1:200; Sigma, MO, USA) or goat anti-rabbit TRITC (1:200; Sigma, MO, USA). The cells were counterstained with DAPI for 3 min and washed with PBS at least three times. Imaging was performed using the Zeiss Axio Imager A1 fluorescence microscope.

Statistical analysis

The Data are expressed as the mean ± standard deviation and analysed using the one-tailed Student's t-test. Statistical significance was determined with P-values less than 0.001 or 0.05, which was specified each time.

Conclusions

In conclusion, our primary studies found that GQDs uptake occurs in a concentration- and time-dependent manner *via* endocytosis. The finding not only offered insights into the underlying uptake mechanisms but also provided important information toward the development of carbon nanoparticle probes for intracellular imaging application. Moreover, we also demonstrated that GQDs internalization did not affect cell viability, proliferation, metabolism, and differentiation, suggesting that GQDs might be biocompatible with hNSCs. Taken together, these findings represent an original investigation of the labeling of stem cells with GQDs and suggest that GQDs may be an effective and eco-friendly probe with low-toxicity for biomedical imaging.

Acknowledgements

This work was supported by the China National Science Foundation (81173139), the Major Research Plan of NSFC (21233003), and the National Key Technology R&D Program (2008BAI49B04).

Notes and references

[a] *Department of Chemistry, Beijing Normal University, Beijing, 100875, China. E-mail: hanmei@bnu.edu.cn; lzfan@bnu.edu.cn*
[b] *Key Laboratory of Cell Proliferation and Regulation Biology, Ministry of Education, Beijing Normal University, Beijing, 100875, China*.

1. K. S. Novoselov, A. K. Geim, S. V. Morozov, D. Jiang, Y. Zhang, S. V. Dubonos, I. V. Grigorieva and A. A. Firsov, *Science*, 2004, **306,** 666-669.
2. K. P. Loh, Q. Bao, G. Eda and M. Chhowalla, *Nat. Chem.*, 2010, **2,** 1015-1024.
3. A. K. Geim and K. S. Novoselov, *Nat. Mater.*, 2007, **6,** 183-191.
4. X. Huang, X. Qi, F. Boey and H. Zhang, *Chem. Soc. Rev.*, 2012, **41,** 666-686.
5. K. Yang, L. Feng, X. Shi and Z. Liu, *Chem. Soc. Rev.*, 2013, **42,** 530-547.
6. K. A. Ritter and J. W. Lyding, *Nat. Mater.*, 2009, **8,** 235-242.
7. J. Peng, W. Gao, B. K. Gupta, Z. Liu, R. Romero-Aburto, L. Ge, L. Song, L. B. Alemany, X. Zhan, G. Gao, S. A. Vithayathil, B. A. Kaipparettu, A. A. Marti, T. Hayashi, J.-J. Zhu and P. M. Ajayan, *Nano Lett.*, 2012, **12,** 844-849.
8. J. Shen, Y. Zhu, X. Yang and C. Li, *Chem. Commun.*, 2012, **48,** 3686-3699.
9. S. J. Zhu, J. H. Zhang, X. Liu, B. Li, X. F. Wang, S. J. Tang, Q. N. Meng, Y. F. Li, C. Shi, R. Hu and B. Yang, *RSC Adv.*, 2012, **2,** 2717-2720.
10. L. L. Li, G. H. Wu, G. H. Yang, J. Peng, J. W. Zhao and J. J. Zhu, *Nanoscale*, 2013, **5,** 4015-4039.
11. Y. Wang, L. Zhang, R. P. Liang, J. M. Bai and J. D. Qiu, *Anal. Chem.*, 2013, **85,** 9148-9155.
12. S. Zhu, J. Zhang, C. Qiao, S. Tang, Y. Li, W. Yuan, B. Li, L. Tian, F. Liu, R. Hu, H. Gao, H. Wei, H. Zhang, H. Sun and B. Yang, *Chem. Commun.*, 2011, **47,** 6858-6860.
13. V. Gupta, N. Chaudhary, R. Srivastava, G. D. Sharma, R. Bhardwaj and S. Chand, *J. Am. Chem. Soc.*, 2011, **133,** 9960-9963.
14. S. Zhuo, M. Shao and S. T. Lee, *ACS Nano*, 2012, 6, 1059-1064.
15. J. Shen, Y. Zhu, C. Chen, X. Yang and C. Li, *Chem. Commun.*, 2011, **47,** 2580-2582.
16. M. Nurunnabi, Z. Khatun, K. M. Huh, S. Y. Park, D. Y. Lee, K. J. Cho and Y. K. Lee, *ACS Nano*, 2013, **7,** 6858-6867.
17. M. Zhang, L. Bai, W. Shang, W. Xie, H. Ma, Y. Fu, D. Fang, H. Sun, L. Fan, M. Han, C. Liu and S. Yang, *J. Mater. Chem.*, 2012, **22,** 7461-7467.
18. J. Peng, S. Wang, P. H. Zhang, L. P. Jiang, J. J. Shi and J. J. Zhu, *J. Biomed. Nanotechnol.*, 2013, **9,** 1679-1685.
19. Q. Liu, B. Guo, Z. Rao, B. Zhang and J. R. Gong, *Nano Lett.*, 2013, **13,** 2436-2441.
20. X. T. Zheng, A. Than, A. Ananthanaraya, D.-H. Kim and P. Chen, *ACS Nano*, 2013, **7,** 6278-6286.
21. L. Deng, L. Liu, C. Zhu, D. Li and S. Dong, *Chem. Commun.*, 2013, **49,** 2503-2505.
22. J. X. Zhao, X. Wu, F. Tian, W. Wang, J. Chen and M. Wu, *J. Mater. Chem. C*, 2013, **1,** 4676-4684.
23. Z. Qian, J. Ma, X. Shan, L. Shao, J. Zhou, J.-R. Chen and H. Feng, *RSC Adv.*, 2013, **3,** 14571-14579.
24. O. Lindvall and Z. Kokaia, *Nature*, 2006, **441,** 1094-1096.
25. S. J. Sharkis, R. J. Jones, C. Civin and Y. Y. Jang, *Sci. Transl. Med.*, 2012, **4,** 127-129.
26. S. Hellman, L. Botnick and P. Mauch, *J. Clin. Oncol.*, 2008, **26,** 821-822.
27. M. Ronaghi, S. Erceg, V. Moreno-Manzano and M. Stojkovic, *Stem Cells*, 2010, **28,** 93-99.
28. V. F. Segers and R. T. Lee, *Nature*, 2008, **451,** 937-942.
29. M. A. Hussain and N. D. Theise, *Lancet*, 2004, **364,** 203-205.
30. T. K. Kuo, S. P. Hung, C. H. Chuang, C. T. Chen, Y. R. V. Shih, S. C. Y. Fang, V. W. Yang and O. K. Lee, *Gastroenterology*, 2008, **134,** 2111-2121.
31. R. Cancedda, G. Bianchi, A. Derubeis and R. Quarto, *Stem Cells*, 2003, **21,** 610-619.
32. C. S. Chen, S. Soni, C. Le, M. Biasca, E. Farr, E. Y. Chen and W. C. Chin, *Nanoscale Res. Lett.*, 2012, **7,** 126.
33. D. L. Clarke, C. B. Johansson, J. Wilbertz, B. Veress, E. Nilsson, H. Karlstrom, U. Lendahl and J. Frisen, *Science*, 2000, **288,** 1660-1663.
34. J. Zhu, L. Zhou and F. XingWu, *N. Engl. J. Med.*, 2006, **355,** 2376-2378.
35. A. Bithell and B. P. Williams, Clin. Sci. (Lond), 2005, **108,** 13-22.
36. Z. Wang, J. Ruan and D. X. Cui, *Nanoscale Res. Lett.*, 2009, **4,** 593-605.
37. J. Ruan, J. J. Ji, H. Song, Q. R. Qian, K. Wang, C. Wang and D. X. Cui, *Nanoscale Res. Lett.*, 2012, **7.**
38. L. Ferreira, J. M. Karp, L. Nobre and R. Langer, *Cell Stem Cell*, 2008, **3,** 136-146.
39. T. Schroeder, *Nature*, 2008, **453,** 345-351.
40. R. Guzman, N. Uchida, T. M. Bliss, D. He, K. K. Christopherson, D. Stellwagen, A. Capela, J. Greve, R. C. Malenka and M. E. Moseley, *Proc. Natl. Acad. Sci.*, 2007, **104,** 10211-10216.
41. S. Lin, X. Xie, M. Patel, Y.-H. Yang, Z. Li, F. Cao, O. Gheysens, Y. Zhang, S. Gambhir and J. Rao, *BMC Biotechnol.*, 2007, **7,** 67.
42. J. K. Hsiao, M. F. Tai, H. H. Chu, S. T. Chen, H. Li, D. M. Lai, S. T. Hsieh, J. L. Wang and H. M. Liu, *Magn. Reson. Med.*, 2007, **58,** 717-724.
43. F. Wang, I. Lee, N. Holmström, T. Yoshitake, D. Kim, M. Muhammed, J. Frisen, L. Olson, C. Spenger and J. Kehr, *Nanotechnology*, 2006, **17,** 1911.
44. J. Ruiz‐Cabello, P. Walczak, D. A. Kedziorek, V. P. Chacko, A. H. Schmieder, S. A. Wickline, G. M. Lanza and J. W. Bulte, *Magn. Reson. Med.*, 2008, **60,** 1506-1511.
45. M. R. Pickard, P. Barraud and D. M. Chari, *Biomaterials*, 2011, **32,** 2274-2284.
46. A. Rak-Raszewska, M. Marcello, S. Kenny, D. Edgar, V. Sée and P. Murray, *PloS one*, 2012, **7,** e32650.
47. L. Ye, K.-T. Yong, L. Liu, I. Roy, R. Hu, J. Zhu, H. Cai, W.-C. Law, J. Liu and K. Wang, *Nat. Nanotechnol.*, 2012, **7,** 453-458.
48. W. Liu, M. Howarth, A. B. Greytak, Y. Zheng, D. G. Nocera, A. Y. Ting and M. G. Bawendi, *J. Am. Chem. Soc.*, 2008, **130,** 1274-1284.
49. K. Kostarelos, L. Lacerda, G. Pastorin, W. Wu, S. Wieckowski, J. Luangsivilay, S. Godefroy, D. Pantarotto, J. P. Briand, S. Muller, M. Prato and A. Bianco, *Nat. Nanotechnol.*, 2007, **2,** 108-113.
50. T. B. Potocky, A. K. Menon and S. H. Gellman, *J. Biol. Chem.*, 2003, **278,** 50188-50194.

51. Z. M. Markovic, B. Z. Ristic, K. M. Arsikin, D. G. Klisic, L. M. Harhaji-Trajkovic, B. M. Todorovic-Markovic, D. P. Kepic, T. K. Kravic-Stevovic, S. P. Jovanovic, M. M. Milenkovic, D. D. Milivojevic, V. Z. Bumbasirevic, M. D. Dramicanin and V. S. Trajkovic, *Biomaterials*, 2012, **33,** 7084-7092.
52. W. A. Hild, M. Breunig and A. Goepferich, *Eur. J. Pharm. Biopharm.*, 2008, **68,** 153-168.
53. Y. Wang, Q. Wu, K. Sui, X. X. Chen, J. Fang, X. Hu, M. Wu and Y. Liu, *Nanoscale*, 2013, **5,** 4737-4743.
54. X. Zhang, W. Hu, J. Li, L. Tao and Y. Wei, *Toxicol. Res.*, 2012, **1,** 62-68.
55. K. Wang, J. Ruan, H. Song, J. Zhang, Y. Wo, S. Guo and D. Cui, *Nanoscale Res. Lett.*, 2011, **6.** 8.
56. J. A. Kim, C. Åberg, A. Salvati and K. A. Dawson, Role of cell cycle on the cellular uptake and dilution of nanoparticles in a cell population, *Nat. Nanotechnol.*, 2012, **7,** 62-68.
57. R. Sakhtianchi, R. F. Minchin, K. B. Lee, A. M. Alkilany, V. Serpooshan and M. Mahmoudi, *Adv. Colloid Interface Sci.*, 2013, **201,** 18-29.
58. Y. Liu, R. Lacson, J. Cassaday, D. A. Ross, A. Kreamer, E. Hudak, R. Peltier, D. McLaren, I. Munoz-Sanjuan, F. Santini, B. Strulovici and M. Ferrer, *J. Biomol. Screen*, 2009, **14,** 319-329.
59. E. Mooney, P. Dockery, U. Greiser, M. Murphy and V. Barron, *Nano Lett.*, 2008, **8,** 2137-2143.
60. S. Y. Park, J. Park, S. H. Sim, M. G. Sung, K. S. Kim, B. H. Hong and S. Hong, *Adv. Mater.*, 2011, **23,** 263-267.
61. J. P. Frimat, J. Sisnaiske, S. Subbiah, H. Menne, P. Godoy, P. Lampen, M. Leist, J. Franzke, J. G. Hengstler and C. van Thriel, *Lab Chip*, 2010, **10,** 701-709.

